

Research Paper

Static Structural Analysis of Checking Fixture Frame of Car Interior Using Finite Element Method

Hanif Setya Hanandita¹, Ubaidillah^{1,2}✉, Aditya Rio Prabowo¹, Bhre Wangsa Lenggana^{1,3}, Arjon Turnip⁴, Endra Joeliyanto⁵

¹Department of Mechanical Engineering, Faculty of Engineering, Universitas Sebelas Maret, 57126 Surakarta, Indonesia

²Department of Mechanical Engineering, Faculty of Engineering, Islamic University of Madinah, Al Madinah Al Munawwarah, 42351, Saudi Arabia

³PT. Bengawan Teknologi Terpadu, Km. 6.5, Wonorejo, Gondangrejo, Jawa Tengah, Karanganyar, 65132, Indonesia

⁴Department of Electrical Engineering, Universitas Padjadjaran, Sumedang 45363, Indonesia

⁵Instrumentation and Control Research Group, Faculty of Industrial Technology, Institut Teknologi Bandung, Bandung 40132, Indonesia

✉ ubaidillah_ft@staff.uns.ac.id

🌐 <https://doi.org/10.31603/ae.9860>



Published by Automotive Laboratory of Universitas Muhammadiyah Magelang collaboration with Association of Indonesian Vocational Educators (AIVE)

Abstract

Article Info

Submitted:

10/08/2023

Revised:

04/12/2023

Accepted:

27/12/2023

Online first:

28/12/2023

An inspection is the most important step for the manufacturers producing their cars. This ensures the seamless compatibility of each car part, as even minor errors can lead to user discomfort during operation. To achieve that goal, the utilization of inspection tools, such as a checking fixture is essential. In this research, we will study the structure analysis of a checking fixture with Ansys software. This study aims to examine the structural strength by analyzing the impact of various design variations on the overall strength outcomes. The requirement for checking fixture is that it must meet the datum tolerance of the car with value of ± 2 mm. Due to that factor, a rigid checking fixture is needed for inspecting the part without experiencing significant deformation. In static loading, the result of the first variation frame has a stress of 5.71 MPa and deformation of 0.051 mm, the second variation frame has a stress of 6.16 MPa and deformation of 0.049 mm and the third variation frame has a stress of 5.63 MPa and deformation 0.042 mm. In terms of weight, the first variation structure has 2470.48 kg, the second variation structure has 2179.93 kg and the third variation structure has 2210 kg. The second variation frame has the highest stress but it has the lightest weight, and the third variation frame has lower stress and deformation but it has a heavier weight than the second variation model. The study results that the second variation model is superior because it has the lightest weight while the three designs have small stress and deformation that still satisfy the requirement of the fixture.

Keywords: Static analysis; FEM; FEA; Checking fixture; Finite element

1. Introduction

Currently, there are many variations in the shape of the vehicle [1]. This is because the vehicle has the major role of transportation and is used by individuals or the public. In 2021, more than 50 million cars were produced, and the quality inspection of car manufacturing must be maintained because it affects the performance and

comfort of the vehicle being made [2]. Quality inspections are conducted throughout the production and assembly processes of the part. In mass production, a sampling method is employed wherein multiple parts are inspected to gauge production capability. This process necessitates the use of checking fixtures, which play a crucial role in terms of cost, quality, and efficiency [3].



This work is licensed under a Creative Commons Attribution-NonCommercial 4.0 International License.

Checking fixture is a component used in the manufacturing process of a vehicle that supports and holds parts in their position [4]. This tool enhances both the productivity and precision of a part, ensuring optimal achievement of product dimensions and geometry while minimizing the risk of failure [5]. Inspecting parts or assembly components, offering a faster alternative to repetitive checks compared to traditional coordinate measurement machines (CMM). Comprising pins, locators, a base, frame, and coordinate lines, a checking fixture is utilized for measuring a part's surface, holes, or shape. During the inspection process, it is crucial for the component to remain stable in its predetermined position. The checking fixture must withstand fatigue to prevent checking inaccuracies caused by loading from the locator and the body where the car part will be installed. Poor checking fixture design is the main cause of inaccurate components that can affect the rejection of the component [6]. In order to avoid that impact, it is necessary to analyze the strength of the checking fixture structure before installing the part, aiming to identify and address any deformations that may occur. This analysis is crucial, as the checking fixture structure plays a pivotal role in supporting all installed components.

After conducting analysis, it is necessary to inspect the manufacturing process of a checking fixture. Inspections in the industrial realm are carried out in the Quality Control process using a CMM (coordinate measuring machine). The CMM serves as a precision measurement tool for assessing the physical geometry of a part. Comprising three main components—mechanical machine, measuring probe, and computing system—the CMM operates on a distinct concept from CNC machines, wherein the tool is moved to generate coordinates along the X, Y, and Z axes [5]. A well-designed checking fixture can produce X, Y, and Z coordinates that align with the 3D design.

In the highly competitive and rapidly evolving landscape of automobile manufacturing, ensuring the highest standards of quality is paramount. Quality control plays a pivotal role in the production process, encompassing a range of systematic measures and inspections to guarantee that each vehicle meets stringent criteria for safety, reliability, and performance. One integral

component of quality control in automobile production is the utilization of checking fixtures. Checking fixtures are specialized tools designed to verify the accuracy and precision of various components during different stages of the manufacturing process. These fixtures are custom-built to match the exact specifications of the automobile parts they assess, providing a consistent and reliable means of quality assurance. The intricate nature of modern automotive designs demands meticulous attention to detail, making checking fixtures indispensable in achieving and maintaining the desired levels of product quality. In the context of automobile production, checking fixtures serve multiple purposes. Firstly, they aid in validating the dimensional accuracy of components, ensuring that each part conforms to the precise specifications outlined in the design phase. This is crucial for guaranteeing the seamless assembly of various parts, reducing the likelihood of defects, and enhancing the overall performance and safety of the vehicle. Secondly, checking fixtures contribute significantly to the detection and prevention of defects in the manufacturing process. By identifying deviations from the specified tolerances early on, manufacturers can implement corrective measures promptly, minimizing the chances of defective products reaching the end of the production line. This proactive approach not only safeguards the reputation of the automobile manufacturer but also enhances customer satisfaction by delivering products that meet or exceed expectations [5], [6].

Moreover, checking fixtures play a pivotal role in streamlining the production process. By providing a standardized and efficient means of quality control, manufacturers can reduce the time and resources required for manual inspections, thereby increasing overall productivity. This is particularly relevant in an industry where precision and efficiency are paramount [6], [7].

In the manufacturing of checking fixtures, many companies often overlook the critical analysis of the structure's strength to determine its adequacy in supporting all installed components. This oversight can lead to geometric disparities between the inspection results using the checking fixture and the original design if the structure cannot adequately handle the current load.

Conversely, overbuilding the frame can result in unnecessary material wastage. This can be avoided by analyzing the finite element method approach, which attempts to lower the possibility of larger losses [7]. The finite element method is a method used to obtain a numerical solution in the world of engineering [8]. The concept of the finite element method is to break large objects into small elements and create relationships between these elements with matrix models that describe the relationships and interactions between elements at a certain point [9].

1.1. Literature Review

Many studies have been conducted on fixture and jig analysis. Arifin, et al. [10] studied fixture frames on the hole-punching tool with a 45-degree angle. This study aims to determine the strength of the structure during loading on the assumption of the compression load of 500 N received during the drilling process. The result obtained stated that the frame was still safe with 145.6 MPa of stress, 0.0194 mm of deformation, and 7.08 of safety factor. Bukkebag, et al. [11] analyzed the fixture for engine block operation. The results of the analysis are in the form of a comparison of the stress acting on the fixture with the yield strength value of the material used. An equivalent Von-Mises stress of 87.44 MPa is acting on the bracket and a maximum principal stress of 88.96 MPa is acting on the height bracket. The results obtained are still safe because the working stress is still below the yield strength of the material used, namely steel with a value of 250 MPa. Siwadamrongpong, et al. [12] investigated the jig structure for bus frames. The research produced data in the form of maximum stress, maximum deformation, and safety factors acting on the jig while supporting the load in the form of a bus frame sub-assembly. The result obtained is still safe because of low deformation and high safety factor with 36.42 MPa of stress, 0.18 mm of deformation, and 10.71 of safety factor. While CAO, et al. [13] examined the fixture for the assembly of aircraft components. The results of this study are in the form of deformation and stress data on the fixture during static condition and with the workload. In static condition, the result obtained the stress of 68.6 MPa and the deformation of 0.144 mm on X axis, 0.288 mm on Y axis, and 0.175 mm on Z axis. In under a working load of 300 N acting during drilling process, the result obtained 79.3 MPa of stress and

the deformation of 0.146 mm on X axis, 0.296 mm on Y axis and 0.509 mm on Z axis. In his research, an optimal fixture design was also produced based on the results of the analysis by considering the critical point, allowable stress and allowable deformation.

Stojadinovic, et al. conducted a study about the inspection process of the object [14]. He investigated the inspection process using digital twins based on CMM. DEA-IOTA-2203 was used as a measurement system and PTC Creo software was used as a modelling software. The research gives the insight into true condition of the object for pre-set tolerance. The measurement result of the object in his research gives an idea to the operator whether the object still needs to be finished or not.

Despite numerous studies focusing on jigs and fixtures in the manufacturing process, the equally crucial role of checking fixtures in ensuring precision has been overlooked. This study seeks to address this gap by examining how the structure of checking fixtures responds to varying loads under different design configurations and how the performance of structure design affects the inspection on CMM at first variation design, which is the structure made.

1.2. Definition of Checking Fixture

A checking fixture is a component used in the manufacturing process of a vehicle that supports and holds parts in their position [3]. Its primary purpose is to verify whether the produced object aligns with specified tolerances, determining its acceptability. According to Hoffman [4] in his book, *Jig and Fixture Design*, the purpose of designing a check tool is to improve quality and production. To achieve that, some criteria must be met: tools can be easily and efficiently operated, reduce costs in producing tools, make tools that can consistently produce high-quality goods, can increase production yields, use materials that can last a long time, and not endanger the safety of the tool operator.

In the process of making a checking fixture design, the designer receives duplicate blueprints of the part to be manufactured. Blueprints can be paper prints or 3D designs. The designer must be able to comprehend the information that is currently available and adhere to the parameters that can impact the form tool design, including the part's overall size and shape, critical components

that demand tight tolerances, and the clamping location on the part's surface. Checking fixtures can be used with several measuring devices, ensuring the part being inspected remains securely in a predetermined position, such as locator, clamp, bushing, and bracket as shown in [Figure 1](#).

The locator is a support component when the car's part is checked. The locator has direct contact with the part because the locator has a function to keep the part in position according to its actual position when the part is used. In some circumstances, the locator may not perform proper support of objects by itself. To keep the part from moving position, a clamp is needed. The clamp operates to apply compressive force to the part's surface, ensuring optimal support on the opposite side through the locator. Bushings are tubular components made using hardened steel. The bushing on the checking fixture functions to ensure that the part of the checking tool in the form of a check pin can correctly measure the part. The inner diameter of the bushing is meticulously designed with a small tolerance to the check pin, ensuring a parallel alignment during the inspection of parts. The bracket is the part that supports the locator or clamp on the checking fixture. In small fixture models, several components such as clamps or locators can be directly attached to the body or frame using bolts. However, in complex and large fixture models, the bracket can have a multipart form to connect the checking fixture components to the frame.

1.3. Coordinate Measurement Machine

In the automotive industry, numerous standards mandate enhanced precision in the

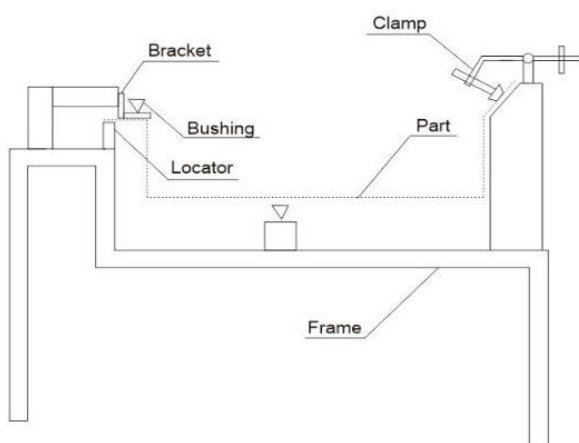


[Figure 1](#). Measuring device on checking fixture

measurement of manufactured components that cannot be done using manual measurement tools. To accelerate the test results, it is necessary to upgrade from manual measurement to digital measuring using a coordinate measuring machine as shown in [Figure 2](#). Coordinate measuring machine is a tool to measure the physical geometry of an object being made. CMM works mechanically by moving the probe to measure the position of the coordinates that have been determined on the object. The probe on the CMM can be a laser or optical which works based on the x,y,z axis. CMM can be used for inspecting manufactured objects as well as in the process of reverse engineering. In its structure, CMM has 3 main components used in making a measurement: the mechanical component that drives the tool, the probe and the computing system that contains the software.

1.4. Finite Element Method

The finite element method is the numerical approach used to obtain a numerical solution to an engineering problem. Many problems such as stress analysis, heat transfer, fluid flow, and electric field have been solved using the finite element method [\[15\]](#). The concept of the finite element method is dividing geometry into multiple elements to calculate multiple values displacement at each node (node point) so that a solution is obtained. This method is used as an analytical tool to solve engineering problems because of the degree of flexibility in distinguishing irregular domains from finite elements. In general, FEA uses three types of analysis, namely, 1D modeling to solve beam, rod,



[Figure 2](#). Coordinate Measurement Machine

and frame elements; 2D modeling, which is useful for solving field-stress and plane-strain problems; and 3D modeling, which is useful for solving complex solid structures [16]. Modern engineering FEA software such as Ansys was extensively applied for rapid analysis [17]. It can produce comprehensive result data and physical response at any location [18]. The widespread use of digital computers and simulation is having a profound effect on engineering and science in today's 4th Industrial Revolution mainly due to the computer hardware, and the appropriate software, for modeling and analyzing complex physical systems and problems [19].

The steps in the finite element method include the preprocessing phase, solution phase, and postprocessing phase. In the preprocessing phase, a model is defined based on the arrangement of geometry, materials, and element shapes which are divided into nodal and elemental forms, and mathematical equations based on the boundary conditions that are made. Furthermore, the Solution Phase stage simultaneously solves the mathematical equations that have been made in the previous stage based on predetermined boundary conditions. The postprocessing Phase stage displays the results of the completion of mathematical equations. The results of these equations are displayed in the form of legend colors, curves, and the vector direction of the force.

In static analysis, the basic equation of motion is using the finite element method of elastic mechanics, as formulated by Eq.(1) [20]. The applied load is not affected by time so the mass matrix and damping matrix are considered zero.

$$[M] \frac{d^2x}{dt^2} + [C] \frac{dx}{dt} + [K]x = F(t) \quad (1)$$

where M is mass matrix, C is damping matrix and K is stiffness matrix. To obtain the result of the displacement then do the inverse of stiffness matrix on both side, as expressed by Eqs. (2) and (3) [21].

$$[K]^{-1}[K]x = F(t) [K]^{-1} \quad (2)$$

$$X = [K]^{-1}F \quad (3)$$

1.5. Materials Response

Under loading conditions, each material has a different response due to its properties. In

industrial, material selection is essential which aims to make the material durable based on its intended function. Within the material, the elastic module has a significant impact on its elasticity. Elasticity modules were obtained from derived between stress and stretch data. Stress is force acting divided by cross-sectional area [22]. Stress can be found using Eq. (4).

$$\sigma = \frac{F}{A} \quad (4)$$

where σ is stress, F is the force that acting on the object, and A is a cross sectional area that is affected by force. While a deformation of an object can be generated using Hooke's law with Eqs. (5) and (6).

$$E = \frac{\sigma}{\varepsilon} \quad (5)$$

$$\varepsilon = \frac{\delta}{L} \quad (6)$$

where E is modulus of elasticity, ε is strain, δ is stretch value and L is initial value.

1.6. Structure Failure Theory

Failure analysis is an analysis performed to determine the cause of the failure. Failure can occur due to static loads and mechanical loads, so stress often arises due to loads that exceed yield strength material. In general, failure theory is divided into three.

1.6.1. Maximum Normal Stress (Rankine Theory)

The failure will occur if the normal tensile stress occurring in the material is equal to or greater than the tensile yield stress material, and failure will occur if the normal compressive stress is less than the compressive yield stress of the material. In general, the maximum normal stress theory [23] is formulated by Eqs. (7) and (8).

$$\sigma_{max} = \frac{\sigma_x + \sigma_y}{2} + \sqrt{\left(\frac{\sigma_x - \sigma_y}{2}\right)^2 + (\tau_{xy})^2} \quad (7)$$

$$FOS = \frac{\sigma_{yp}}{\sigma_{max}} \quad (8)$$

1.6.2. Maximum Shear Stress (Rankine Theory)

This theory states that failure will occur if the shear stress occurring in the material is equal to or greater than the maximum shear stress on yield material conditions. The value of the maximum

shear stress is half of the maximum normal stress value [23], as calculated by Eqs. (9) and (10).

$$\sigma_{max} = \sqrt{\left(\frac{\sigma_x + \sigma_y}{2}\right)^2 + (\tau_{xy})^2} \quad (9)$$

$$FOS = \frac{1}{2} \times \frac{\sigma_{yp}}{\sigma_{max}} \quad (10)$$

1.6.3. Distortion Energy (Von Mises Theory)

This theory is based on determining the distortion energy in a material. The energy distortion theory, also known as the von Mises stress theory, was introduced by Huber and perfected by Richard von Mises in 1883-1953. This theory states that failure will occur if the distortion energy in the material (the energy associated with volume changes in the same material) is equal to or greater than the distortion energy in the yielding material (See Figure 3) [23]. σ_{max} and FOS is calculated by Eqs. (11) and (12).

$$\sigma_{max} = \sqrt{\frac{(\sigma_x - \sigma_y)^2 + (\sigma_y - \sigma_z)^2 + (\sigma_z - \sigma_x)^2}{2}} \quad (11)$$

$$FOS = \frac{\sigma_{yp}}{\sigma_{max}} \quad (12)$$

2. Method

2.1. The Works of Principle

The study commences by validating data from prior research. In the data validation process, the research is conducted in the same manner as in Arifin et al.'s [10] design, utilizing Fusion 360 for designing and Ansys Workbench for simulating the model, as illustrated in Figure 4. Data validation is performed to compare the von Mises stress results between the initial simulation and the latest simulation. The disparity in the data obtained from previous research should not exceed a maximum value of 5%. This is intended to ensure that the conducted simulation is both

accountable and valid. Following the latest simulation, a comparison reveals a deviation of less than 5% when compared to the research conducted by Arifin et al. [10]. Once the data validation process is completed, and the resulting deviation is known, the subsequent step involves collecting data using the initial and optimized designs of the checking fixture structure.

2.2. Design

The research continued by taking structural analysis data consist of von mises stress, deformation, safety factor and mass from various design structures. The model of the structures can be seen in Figure 5 to Figure 7.

The first design variation employs a double structure member featuring 50 mm x 50 mm hollow carbon steel on the side of the structure. In contrast, the second variation is simplified, utilizing a single structure made of 75 mm x 75 mm hollow carbon steel. The third design variation uses the same size of hollow carbon steel

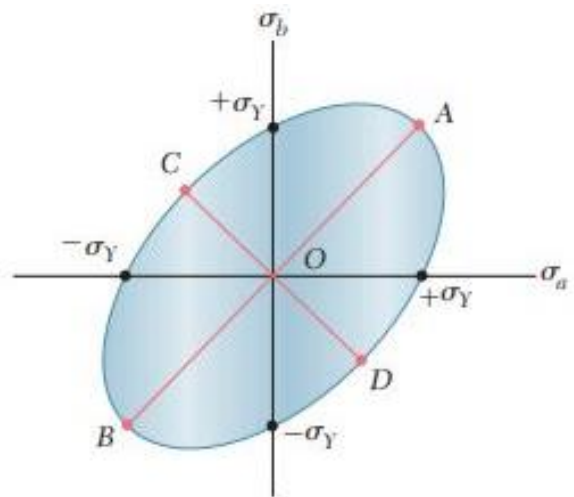


Figure 3. Von mises stress based on energy distortion criteria

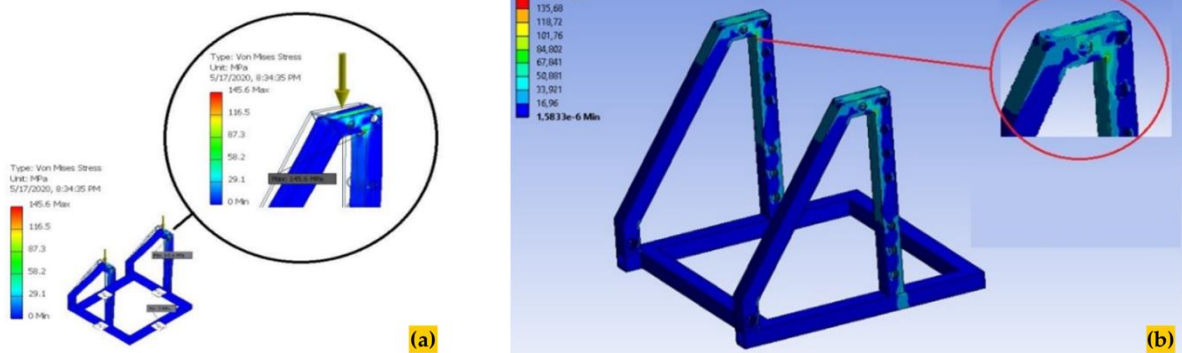


Figure 4. (a) Stress at initial simulation (b) Stress at latest simulation



Figure 5. First variation design structure



Figure 6. Second variation design structure

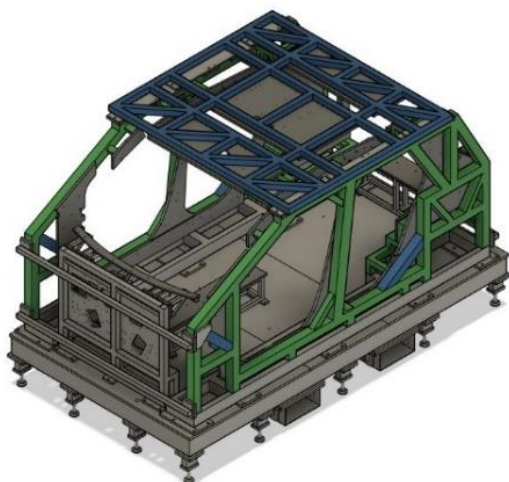


Figure 7. Third variation design structure

as the second variation but integrates reinforcement in both the top and side structures. In the top structure, which previously consisted of

three truss groups in the second variation design, these are amalgamated into a single truss group in the third variation design.

2.3. Materials

The material used for the structure in this study is hollow carbon steel. Carbon steel was chosen in this study because of material properties and ease of obtaining material in the market. Carbon steel offer a proper combination of ductility, toughness, strength and weldability. **Table 1** shows the mechanical properties of carbon steel. The material used to mount the car parts checker is made of bakelit (phenol-formaldehyde resin). Bakelit was chosen because it is easy to shape, easy to machining and heat resistant. The properties of bakelit can be seen in **Table 2**. The material used to check the part of the car geometry is made of Necuron 800. Necuron 800 was chosen because it is easy to shape, easy to machining and heat resistant. The physical properties of this material can be seen in **Table 3**.

2.4. Meshing

Meshing is a crucial step in the finite element method, involving the division of a three-dimensional object into thousands of cells to accurately define its physical shape [24]. In the meshing process, the quality of the mesh used in the analysis directly influences the accuracy of the obtained values and the CPU time required to complete the analysis. For this simulation, the detailed mesh settings include the fast transition, medium smoothing, assembly for the initial seed size, and default defeaturing size. Several parameters, such as aspect ratio, orthogonal quality, and skewness, are considered to assess the mesh quality. To ensure the precision of the study results, a convergence study was conducted to determine the appropriate mesh size. Researchers conduct mesh convergence studies to achieve more accurate results based on the required meshing size [25]. The objective of this study is to identify the correct mesh size, ensuring that the results exhibit minimal change with increasing mesh density. If the results show a small enough change, indicating convergence, the relative error between mesh sizes is calculated as a percentage difference for each output. If increasing mesh density (decreasing element size) does not alter the analysis results by more than

Table 1. Property of hollow carbon steel (PT Krakatau Steel)

Properties	Carbon Steel Hollow	Unit
Tensile strength, ultimate	400	MPa
Tensile strength, yield	245	MPa
Modulus elasticity	210	Gpa
Poisson's ratio	0.29	-
Density	7.85	g/cc

Table 2. Property of bakelit (NECUMER GmbH catalog. 2010)

Properties	Bakelit	Unit
Tensile strength	50	MPa
Compressive strength	250	MPa
Tensile Modulus	7500	MPa
Density	1.42	g/cc

Table 3. Property of Necuron 800 (HEXION GmbH catalog-2010)

Properties	Necuron 800	Unit
Colour	Ivory/grey	-
Coefficient of thermal expansion	Approx, 45×10^{-6}	K ⁻¹
Compressive Strength	Approx. 46	MPa
Flexural Strength	Approx, 61	MPa
Modulus of elasticity	Approx, 1.670	MPa
Density	Approx 1.00	g/cc

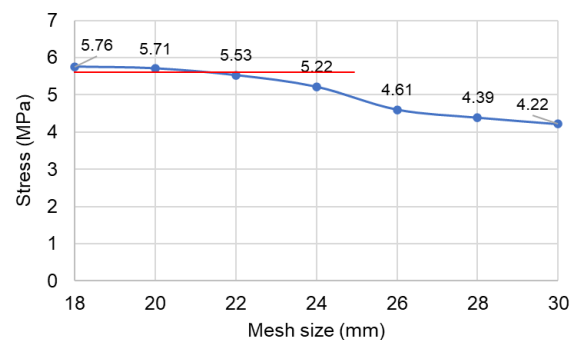
5%, then the mesh size is deemed acceptable [26], [27]. The formula for relative error can be found using Eq. (13), as follows:

$$\text{error relative \%} = \frac{j_{\text{trial}} - (j-1)_{\text{trial}}}{(j-1)_{\text{trial}}} \times 100 \quad (13)$$

Referring to **Figure 8**, it is observed that a mesh size of 20 mm exhibits no significant change in stress values compared to the 18 mm mesh size, with a difference of 0.047 MPa and an error value of 0.82%. Consequently, this study will proceed with a mesh size of 20 mm to enhance computational efficiency, as illustrated in **Figure 9** [28]. The mesh quality value is determined based on the selected mesh size, and its evaluation is conducted using parameters provided by Faturrohman et al. [29]. **Table 4** displays the mesh quality values for the model, demonstrating that the mesh quality falls within the specified limit, as defined by the ideal values established by Faturrohman et al. [29].

Table 4. Mesh quality parameter

Parameter	Value
Skewness	0.654
Aspect Ratio	4.414
Orthogonal Quality	0.351

**Figure 8.** Convergence study

2.5. Boundary Condition

The boundary condition employed for static loading analysis involves securing the lower part of the frame support with a stainless steel adjuster, serving as a fixed support to prevent any movement of the frame. The static load encompasses the weight of the car component attached to the checking fixture. This particular component is constructed from Necuron 800 material. The load applied by the car's part checker on the checking fixture is determined through density calculations for each component. The calculation of the load can be obtained using Eq. (14).

$$m = \rho \times V \quad (14)$$

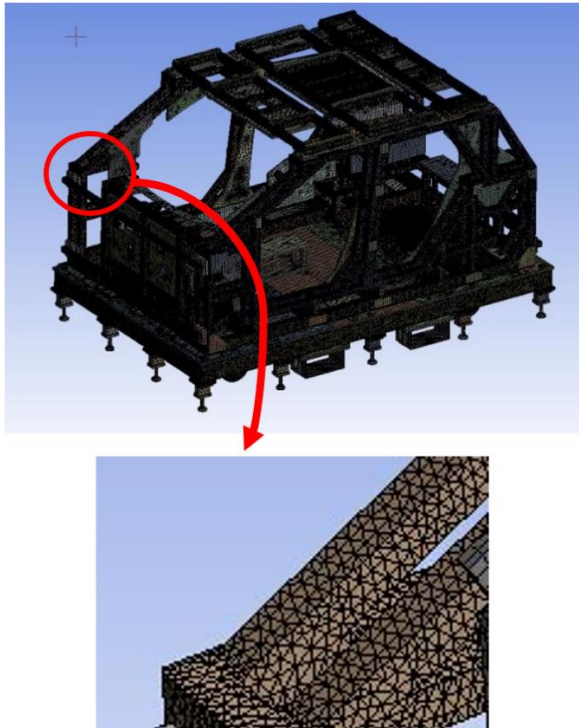


Figure 9. Mesh model (20 mm)

Based on Eq. (14) ρ is density, m is the mass of the object, and V is the volume of the object. The load value of the each components of car's part checker shows in Table 5. Load 1 until 8 has 2 bodies that located on the right and left side of the frame, while the rest has 1 body. The position of each component of car's part checker shows in Figure 10 and Figure 11.

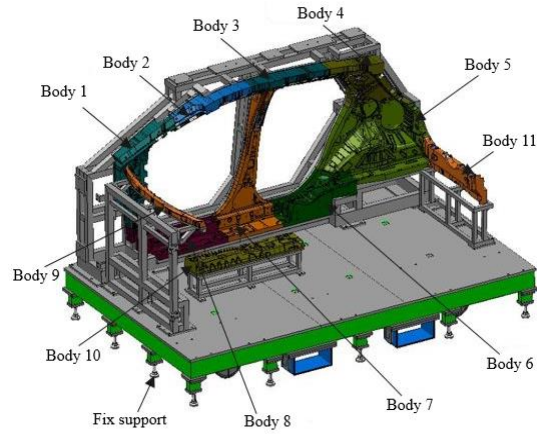


Figure 10. Load at main structure

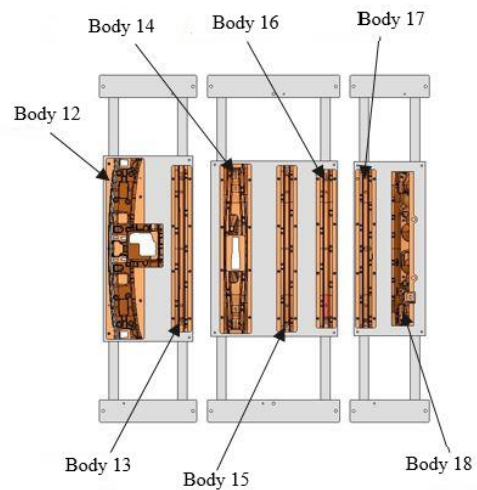


Figure 11. Load at top structure

Table 5. The load value of the component

Load	Volume (cm ³)	Mass (kg)	Amount
1	14.170	14.17	2 (L-R)
2	6.046	6.05	2 (L-R)
3	6.953	6.95	2 (L-R)
4	28.719	28.72	2 (L-R)
5	42.161	42.16	2 (L-R)
6	24.839	24.84	2 (L-R)
7	22.316	22.32	2 (L-R)
8	20.296	20.29	2 (L-R)
9	2.477	2.48	1
10	13.236	13.24	1
11	11.567	11.57	1
12	16.511	16.51	1
13	3.360	3.36	1
14	5.140	5.14	1
15	3.262	3.26	1
16	4.003	4.00	1
17	2.942	2.94	1
18	12.301	12.30	1

3. Results and Discussion

This study aims to design a structure of checking fixtures to hold the car's part checker without experiencing much fatigue. The design concept carried out in this study is to create a new structure design that is lighter than the initial design while still considering the strength of static loading. It is intended to save material costs and reduce weight so that the production of the fixture can be increased and more efficient.

3.1. Static Structural Analysis

Static structural simulation in Ansys Workbench is utilized to assess the strength of the checking fixture structure. In this simulation, the structure is subjected to a continuous static load characterized by a steady-state variable. The sought-after values for this loading scenario include stress (von Mises), deformation, and the safety factor of the structure. Von Mises stress is employed to predict material yield based on the resultant of the three principal stresses. Failure in the von Mises criterion is anticipated if the von Mises stress value exceeds the material's yield stress.

The initial design variation of the checking fixture structure, with dimensions of 50 x 50 mm and a double structure on the right and left sides, yields a stress result of 5.71 MPa at the top right structure's welding joint, as depicted in Figure 12. This stress concentration is significant at the points where the structures intersect. Figure 13 shows a total deformation result of 0.051 mm at the top structure of the checking fixture. This deformation is attributed to the location being distant from the main supporting frame, causing the most substantial deflection under the applied load. The safety factor of the structure exceeds a value of 15.

The second variation design of the checking fixture structure with dimension 75 x 75 mm and using a single structure on the right and left sides obtained the result with a stress of 6.16 MPa at the front right structure at the welding joint as seen in Figure 14. This occurs due to the points where the structures meet each other, resulting in a substantial stress concentration at those locations. The stress value of the second variation structure design has increased the value by 8% compared to the first variation design due to a change in a structure from double to single structure on the

right and left sides that resulting in lower stiffness of the structure and greater stress. In Figure 15, the result obtained the total deformation of 0.049 mm at the top structure. The safety factor of the structure obtained the value of more than 15.

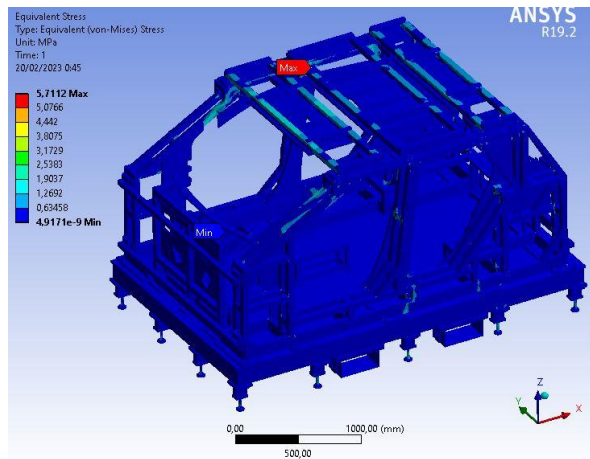


Figure 12. The von mises stress of the first variation

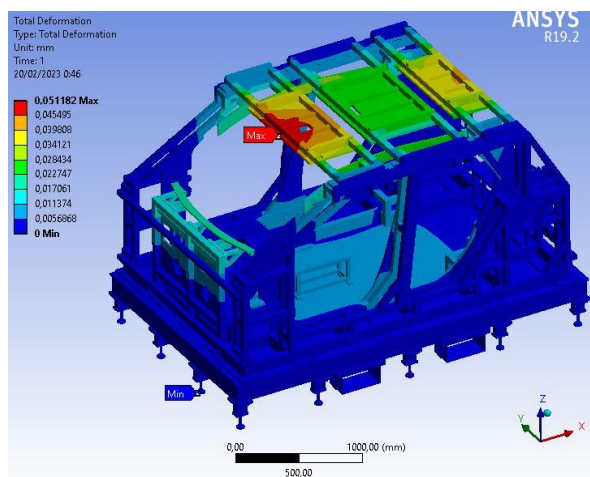


Figure 13. Total deformation of the first variation

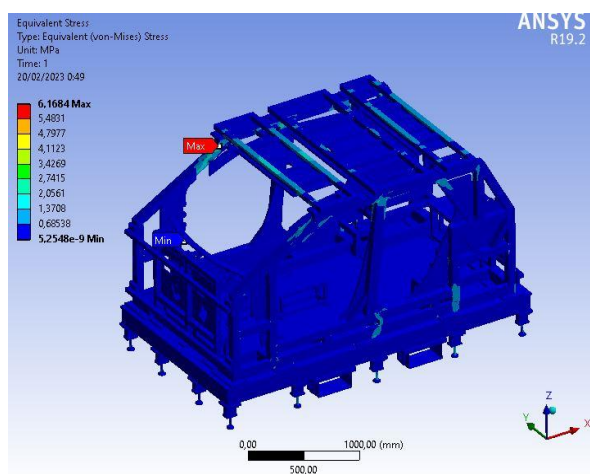


Figure 14. The von mises stress of second variation design

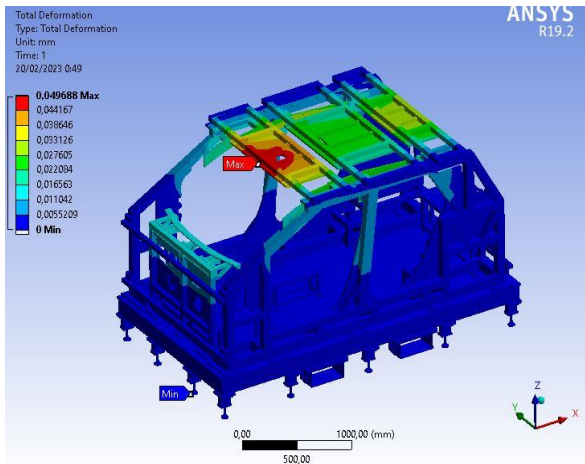


Figure 15. Total deformation of second variation design

The third variation design of the checking fixture structure with dimensions 75 x 75 mm and using a single structure on the right and left structures obtained the result with a stress of 5.63 MPa at the front right structure at the welding joint as seen in Figure 16. The maximum stress point obtained is the same location as in the second variation design. The stress value of the third variation design is lower compared to the second variation design due to the distribution of forces on the third variation design being better with the reinforcement structures on the top and side frames. The stress value of the third variation design has decreased the value by 9.5% compared to the second variation design and decreased the value by 1.3% compared to the first variation design. In Figure 17, the result obtained the total deformation of 0.042 mm at the top structure. The safety factor of the structure obtained a value of more than 15.

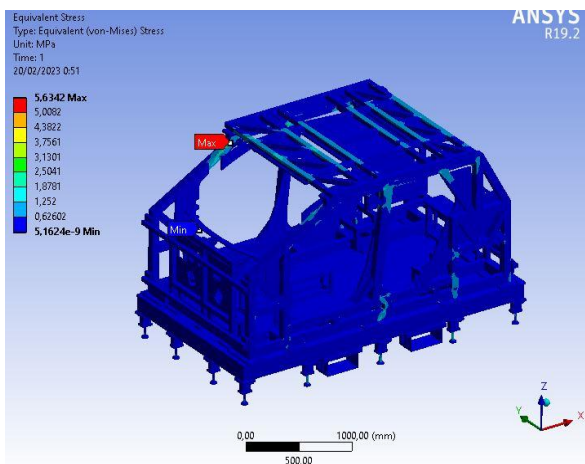


Figure 16. The von mises stress of third variation design

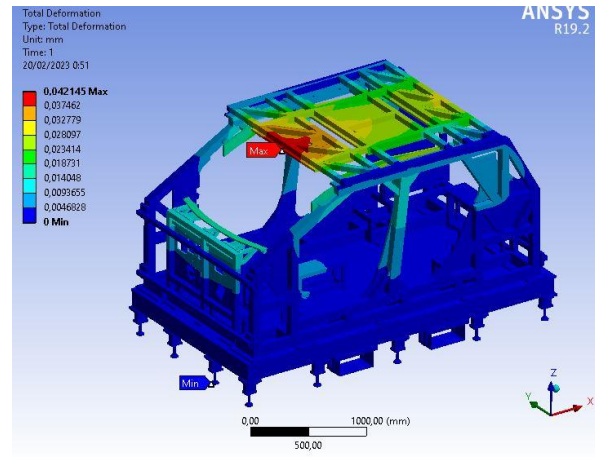


Figure 17. Total deformation of third variation design

3.2. Coordinate Measurement Machine Analysis

The examination of the checking fixture structure with the Coordinate Measurement Machine (CMM) tool is conducted on the initial design variation. CMM measurements are executed using the ROMER Arm machine. The purpose of these measurements is to ascertain whether the manufactured fixture still adheres to the tolerance standards specified by the customer. In this instance, PT. X. with a tolerance of ± 0.2 mm in its actual condition.

In the CMM inspection, the Necuron body component, serving as a load, undergoes geometric position checks to assess the deviation caused by its own load according to the original design. The examination is conducted for each Necuron body, which functions as a mounting point for attaching car parts. This analysis includes a comparison of deformation results obtained from simulation and direct CMM checks conducted along three Cartesian axes, with the Z-axis aligning with the object's height. Table 6 presents the deviations observed in both simulation and CMM checks.

The results indicate that the structure of the initial design complies with the specified tolerance requirements of ± 0.2 mm. The simulations exhibit relatively small deviations, suggesting the potential for simplifying the existing structure to reduce material usage. Discrepancies between FEM simulation and CMM checks are notable due to the latter involving contact with the finished surface, resulting in a slightly different contour from the design.

Table 6 reveals the most significant deformation occurring along the Z-axis, corresponding to the force direction. The

maximum deviation in the simulation is identified at load 12, which shares a holder with load 13 for attachment and is positioned far from the main support structure, leading to substantial deflection. Figure 18 illustrates a comparison of deviations between simulation and CMM checks along the x, y, and z axes.

Figure 19 displays simulation results for body 12, revealing maximum deformations of 0.004 mm on the X-axis, 0.0017 mm on the Y-axis, and 0.049 mm on the Z-axis. Meanwhile, Figure 20 depicts CMM checking results, where position deviations are measured based on the requested datum point. For body 12, deviations occur at rectangle 39 datum, measuring 0.166 mm on the X-axis, 0.173 mm on the Y-axis, and 0.088 mm on the Z-axis. Significant differences in deviation values between simulation and CMM checks are attributed to the machining process of Necuron using a CNC tool, which may not achieve the same accuracy as the design, especially on surface sections. Additionally, manual production of the frame can introduce geometric mismatches between the manufactured frame and the original design.

3.3. Structure Design Analysis

The frame's stresses, deformations and safety factor are obtained based on the color legend. The

first design shows a stress value of 5.71 MPa, a deformation of 0.051 mm and a safety factor of 15. The mass obtained for the first design is 2470.48 kg. The first design results show that the frame is rigid to support the given load, but it is still too heavy. Then in the second design with a mass of 2179.93 kg the stress obtained is 6.16 MPa, with a deformation of 0.049 mm and a safety factor of 15. In the third design, the stress is obtained 5.63 MPa, a deformation of 0.042 mm and safety factor of 15. The mass obtained in the third design is 2210 kg. The stress comparison that occurs in the three design structures is shown in Figure 21.

In static loading, the parameters utilized to assess the effectiveness of the design encompass stress, deformation, safety factor, and mass. Analysis of the simulation, which involves reducing the frame structure in the checking fixture, reveals an increase in stress and deformation acting on the frame. This occurrence is attributed to the diminishing distribution of force to the frame members in proportion to the reduction in members within the checking fixture frame. However, relying solely on stress and deformation parameters is insufficient to determine the optimal design among the three structural types due to the relatively minor differences.

Table 6. Datum value between simulation and CMM

Load	X		Y		Z	
	Simulation	CMM	Simulation	CMM	Simulation	CMM
1	0.0019	0.048	0.001	0.007	0.027	0.038
2	0.0007	0.008	0.009	0.055	0.037	0.088
3	0.0002	0.185	0.011	0.053	0.036	0.039
4	0.0014	0.114	0.019	0.117	0.015	0.008
5	0.0004	0.048	0.0013	0.081	0.004	0.016
6	0.0004	0.109	0.002	0.176	0.005	0.056
7	0.0015	0.191	0.007	0.041	0.007	0.044
8	0.0001	0.16	0.002	0.161	0.005	0.021
9	0.017	0.069	0.007	0.039	0.023	0.057
10	0.001	0.139	9.6x10 ⁻⁶	0.067	0.007	0.006
11	0.003	0.152	8.9x10 ⁻⁶	0.132	0.002	0.033
12	0.004	0.166	0.0017	0.173	0.049	0.088
13	0.0005	-	0.0003	-	0.02	0
14	0.0006	0.089	0.0002	0.181	0.026	0.162
15	0.0003	-	0.0002	-	0.02	0
16	0.0002	-	0.0003	-	0.018	0
17	0.0016	-	0.0002	-	0.018	0
18	0.0035	0.12	0.0025	0.01	0.034	0.067

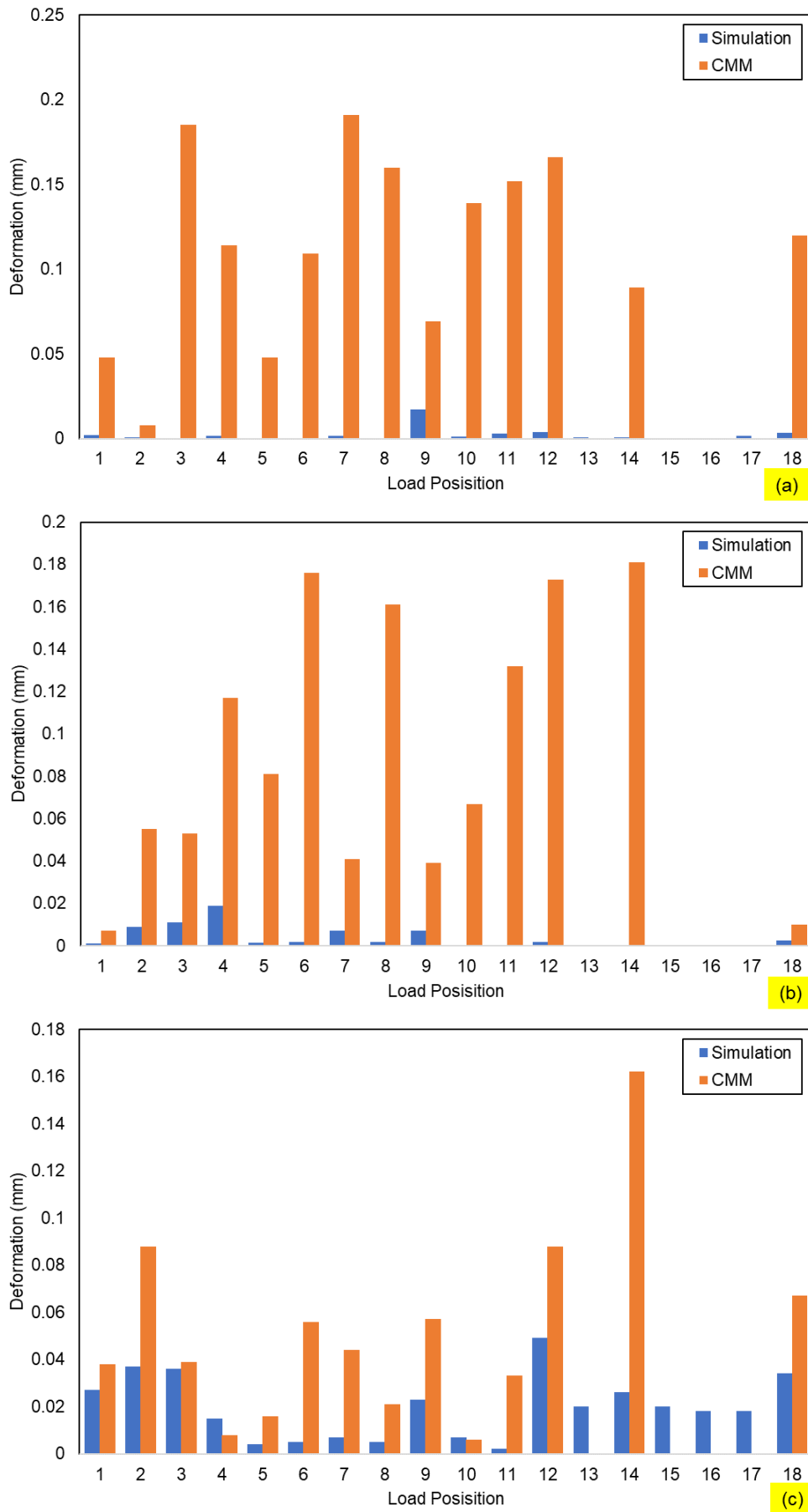


Figure 18. Datum value between simulation and CMM on (a) X. (b) Y and (c) Z axis

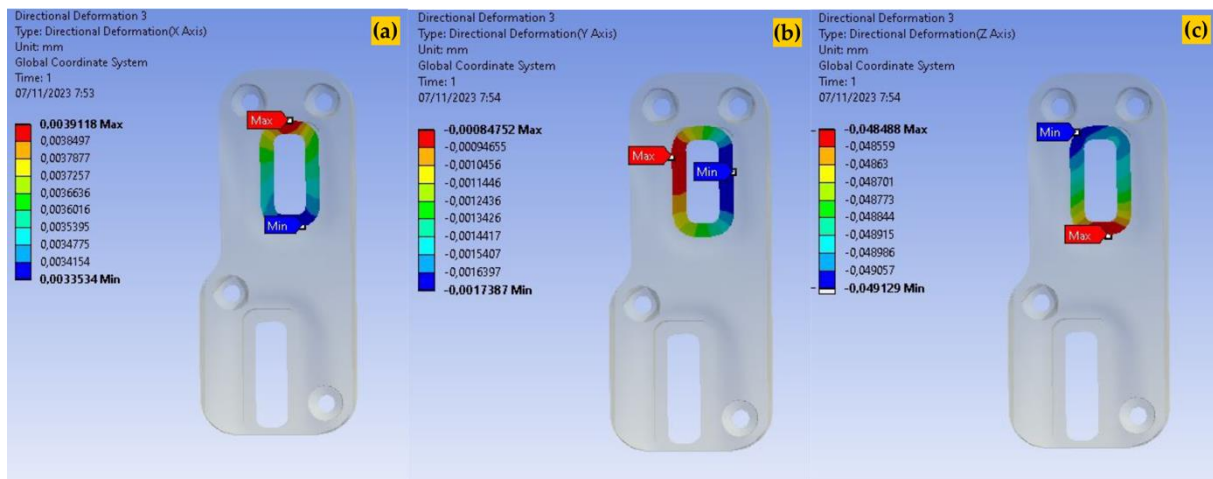


Figure 19. Deformation result on load 12 at (a) X axis. (b) Y axis. dan (c) Z axis

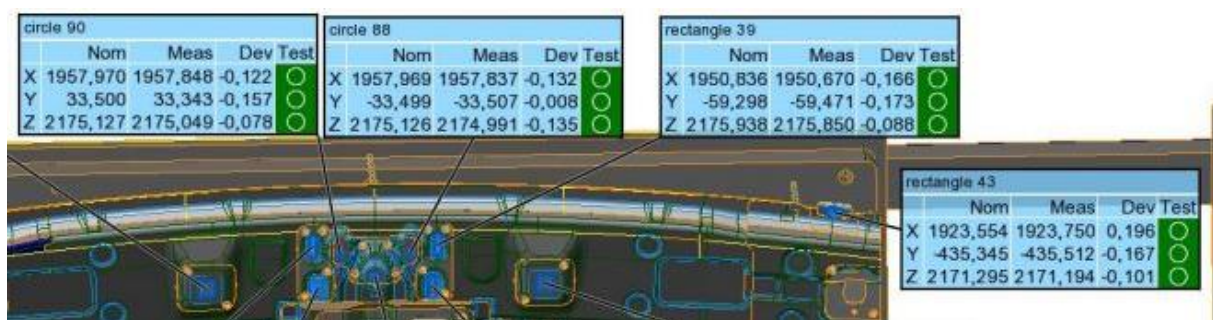


Figure 20. CMM checking on load 12

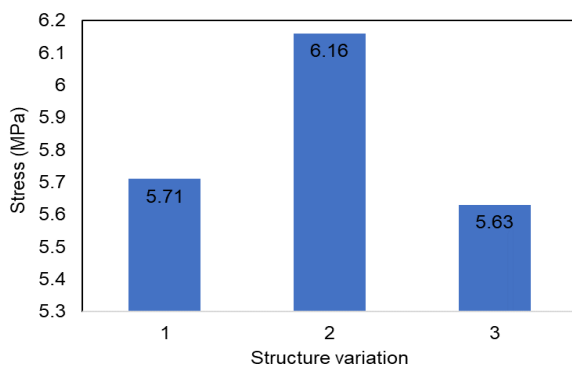


Figure 21. Stress value of three design structures

Therefore, the mass of the design is also taken into account to assess the performance value of the frame. Among the three design structures, the second variation design exhibits the smallest mass, measuring 2179.93 kg. Compared to the first variation design, this represents a decrease in mass of 11.76%. Meanwhile, the third variation design has a mass of 2210 kg, indicating a 1.38% increase compared to the second variation design and a 10.54% decrease compared to the first

variation design. A detailed comparison of the checking fixture frame masses is presented in Table 7.

Overall based on static loading analysis, all design variations can be said to be safe because the working stress is still far below the yield strength value of the material used. the deformation that occurs is still below the tolerance value set by the consumer of ± 0.2 mm and the safety factor value that occurs is still above number 15. Based on the mass parameter, it can be concluded that the second variation design has better performance compared to the two existing design variations because it has the lightest mass so that the cost of making a checking fixture frame can be reduced.

Table 7. Mass comparison between 3 structure

Design Variation	Mass (kg)
First Variation	2470.5
Second Variation	2179.93
Third Variation	2210

4. Conclusion

The static loading analysis of the three variations of the checking fixture frame design has been conducted. The first variation design exhibits a stress value of 5.71 MPa, a deformation of 0.051 mm, and a safety factor of 15. In comparison, the second variation design has a stress value of 6.16 MPa, a deformation of 0.049 mm, and a safety factor of 15. The third variation design features a stress value of 5.63 MPa, a deformation of 0.042 mm, and a safety factor of 15. The CMM checking results for the first variation design remain within the specified tolerance limits, but there is a noteworthy difference in values compared to the simulation results, attributed to the finishing touch on the necuron body. It is recommended that in future analyses, checks should be performed before surface finishing to obtain more accurate values. Among the three design variations, the second variation design demonstrates superior performance when compared to the first and third variation designs. This superiority is evident in a stress value that is 10% lower, a deformation value that is 2.11% lower, and a mass that is 11.76% lower than the first design. Although the third variation design presents lower stress and deformation values than the second variation design, it has a heavier mass than both the first and second variation designs. Considering that all three design variations are deemed safe, the preference is given to the design with a lighter mass, making the second variation design superior.

Acknowledgement

Authors thank to Universitas Sebelas Maret for the funding under scheme Hibah RKI (Riset Kolaborasi Indonesia) 2023.

Author's Declaration

Authors' contributions and responsibilities

The authors made substantial contributions to the conception and design of the study. The authors took responsibility for data analysis, interpretation and discussion of results. The authors read and approved the final manuscript.

Funding

This research was funded by Riset Kolaborasi Indonesia under contract number 590.1/UN27.22/HK.07.00/2023.

Availability of data and materials

All data are available from the authors.

Competing interests

The authors declare no competing interest.

Additional information

No additional information from the authors.

References

- [1] T. A. bin A. Razak, K. S. bin Shafee, K. A. bin Shamsuddin, M. R. bin Ibrahim, and B. T. H. T. bin Baharuddin. "Application of 3D scanning onto automotive door panel for quality." in *2016 International Conference on Robotics and Automation Engineering (ICRAE)*. 2016. pp. 31–34. doi: 10.1109/ICRAE.2016.7738783.
- [2] German Association of the Automotive Industry (VDA). "Statistics of world car production." Berlin. 2022.
- [3] H. Cai-qi, L. Zhong-qin, and L. Xin-min. "Concept design of checking fixture for auto-body parts based on neural networks." *The International Journal of Advanced Manufacturing Technology*, vol. 30, no. 5, pp. 574–577. 2006. doi: 10.1007/s00170-005-0039-4.
- [4] E. G. Hoffman. *Jig and Fixture Design*. United States of America: Delmar Learning. 2011.
- [5] N. Neve and V. Kurkute. "Design and Finite Element Analysis of Differential Multi-Gauging System." *International Journal of Recent Technology and Engineering (IJRTE)*, vol. 8, no. 6, pp. 3250–3254. 2020. doi: 10.35940/ijrte.f7937.038620.
- [6] T. A. bin Abdul Razak, B. T. H. T. bin Baharudin, K. S. bin Shafee, and K. A. bin Shamsuddin. "Application of a Portable Coordinate Measuring Machine onto Automotive Door Panel for Quality Inspection Activity BT - Advanced Engineering for Processes and Technologies." A. Ismail, M. H. Abu Bakar, and A. Öchsner, Eds. Cham: Springer International Publishing. 2019, pp. 25–36.
- [7] Y. Sanjaya, A. R. Prabowo, F. Imaduddin, and N. A. Binti Nordin. "Design and Analysis of Mesh Size Subjected to Wheel Rim Convergence Using Finite Element Method." *Procedia Structural Integrity*, vol. 33, pp. 51–58. 2021. doi: <https://doi.org/10.1016/j.prostr.2021.10.008>.
- [8] R. L. L. Hidayat. *eori dan Penerapan Metode Elemen Hingga*. Surakarta: UNS Press. 2005.

- [9] Y. Basavaraj and P. Kumar. "Modeling and Analysis of Support Pin for Brake Spider Fixture by Fem Using Ansys Software." *IOSR Journal of Mechanical and Civil Engineering*. vol. 6. no. 1. pp. 10–15. 2013. doi: 10.9790/1684-0611015.
- [10] F. Arifin et al.. "Studi analisis simulasi kekuatan beban pada alat bantu pembuatan lubang dengan sudut kemiringan 45 derajat." *Jurnal Polimesin*. vol. 18. no. 2. pp. 116–123. 2020.
- [11] S. Bukkebag and S. R. Basavaraddi. "Design And Finite Element Analysis Of Fixture For Milling Of Cummins Engine Block." *International Research Journal of Engineering and Technology (IRJET)*. vol. 4. no. 8. pp. 2215–2221. 2017. [Online]. Available: <https://irjet.net/archives/V4/i8/IRJET-V4I8400.pdf>.
- [12] S. Siwadamrongpong and U. Ongarjwutichai. "Simulation and design of jigs for bus's chassis production." *International Journal of Mechanics*. vol. 4. no. 4. pp. 87–93. 2010.
- [13] W. Cao. G. L. Zheng. J. L. Xu. and Y. Qiu. "Finite Element Analysis for Assembly Fixtures Based on ANSYS." *Applied Mechanics and Materials*. vol. 380–384. pp. 173–176. 2013. doi: 10.4028/www.scientific.net/AMM.380-384.173.
- [14] S. M. Stojadinovic. V. D. Majstorovic. N. M. Durakbasa. and D. Stanic. "Contribution to the development of a digital twin based on CMM to support the inspection process." *Measurement: Sensors*. vol. 22. p. 100372. 2022. doi: <https://doi.org/10.1016/j.measen.2022.100372>.
- [15] L. W. Prasetya. A. R. Prabowo. Ubaidillah. and N. A. Binti Nordin. "Crashworthiness Analysis of Attenuator Structure based on Recycled Waste Can subjected to Impact Loading: Part I – Absorption Performance." *Procedia Structural Integrity*. vol. 27. pp. 125–131. 2020. doi: <https://doi.org/10.1016/j.prostr.2020.07.017>.
- [16] B. W. Lenggana et al.. "Effects of mechanical vibration on designed steel-based plate geometries: behavioral estimation subjected to applied material classes using finite-element method." vol. 8. no. 1. pp. 225–240. 2021. doi: doi:10.1515/cls-2021-0021.
- [17] I. A. Majid. F. B. Laksono. H. Suryanto. and A. R. Prabowo. "Structural Assessment of Ladder Frame Chassis using FE Analysis: A Designed Construction referring to Ford AC Cobra." *Procedia Structural Integrity*. vol. 33. pp. 35–42. 2021. doi: <https://doi.org/10.1016/j.prostr.2021.10.006>.
- [18] A. K. Ary. A. R. Prabowo. and F. Imaduddin. "Structural assessment of alternative urban vehicle chassis subjected to loading and internal parameters using finite element analysis." *Journal of Engineering Science and Technology*. vol. 15. no. 3. pp. 1999–2022. 2020.
- [19] K. Chong. A. Boreasi. S. Saigal. and J. Lee. *Numerical Methods in Mechanics of Materials*. CRC Press. 2017.
- [20] C. Kashyap. "Vibration Analysis of Structures." National Institute of Technology. Rourkela. 2007.
- [21] H. Patil and P. V. Jeyakarthykeyan. "Mesh convergence study and estimation of discretization error of hub in clutch disc with integration of ANSYS." *IOP Conference Series: Materials Science and Engineering*. vol. 402. no. 1. p. 12065. 2018. doi: 10.1088/1757-899X/402/1/012065.
- [22] D. R. H. Jones and M. F. Ashby. *Engineering Materials 1*. 6th ed. 2019.
- [23] F. P. B. Jr. E. R. Johnston. J. T. Dewolf. and D. F. Mazurek. *Mechanics of Materials*. New York: McGraw-Hill. 2011.
- [24] Y. Crama and P. L. Hammer. "Fundamental concepts and applications." in *Boolean Functions: Theory, Algorithms, and Applications*. Y. Crama and P. L. Hammer. Eds. Cambridge: Cambridge University Press. 2011. pp. 3–66.
- [25] M. Ahmad. K. A. Ismail. and F. Mat. "Convergence of Finite Element Model for Crushing of a Conical Thin-walled Tube." *Procedia Engineering*. vol. 53. pp. 586–593. 2013. doi: <https://doi.org/10.1016/j.proeng.2013.02.075>.
- [26] W. M. Chen. Y. H. Cai. Y. U. E. Yu. X. Geng. and X. I. N. Ma. "Optimal Mesh Criteria In Finite Element Modeling Of Human Foot: The Dependence For Multiple Model Outputs On Mesh Density And Loading Boundary Conditions." *Journal of Mechanics in Medicine and Biology*. vol. 21. no. 9. pp. 1–14. 2021. doi: 10.1142/S0219519421400340.

- [27] A. Z. bin Pokaad. M. Z. M. Nasir. and Ubaidillah. "Simulation and experimental studies on the behavior of a magnetorheological damper under impact loading." in *2011 4th International Conference on Mechatronics (ICOM)*. 2011. pp. 1–7. doi: 10.1109/ICOM.2011.5937114.
- [28] F. H. A. Alwan. A. R. Prabowo. T. Muttaqie. N. Muhayat. R. Ridwan. and F. B. Laksono. "Assessment of ballistic impact damage on aluminum and magnesium alloys against high velocity bullets by dynamic FE simulations." vol. 31. no. 1. pp. 595–616. 2022. doi: doi:10.1515/jmbm-2022-0064.
- [29] N. Fatchurrohman and S. T. Chia. "Performance of hybrid nano-micro reinforced mg metal matrix composites brake calliper: simulation approach." *IOP Conference Series: Materials Science and Engineering*. vol. 257. no. 1. p. 12060. 2017. doi: 10.1088/1757-899X/257/1/012060.